

1        **A new set of composite, non-redundant electroencephalogram**  
2        **measures of non-rapid eye movement sleep based on the power**  
3        **law scaling of the Fourier spectrum**

4        Róbert Bódizs<sup>1,2\*</sup>, Orsolya Szalárdy<sup>1,3</sup>, Csenge Horváth<sup>1</sup>, Péter P. Ujma<sup>1,2</sup>, Ferenc Gombos<sup>4,5</sup>,  
5        Péter Simor<sup>1,6,7</sup>, Adrián Pótári<sup>5,8</sup>, Marcel Zeising<sup>9,10</sup>, Axel Steiger<sup>9</sup>, Martin Dresler<sup>11</sup>

6        <sup>1</sup>Institute of Behavioural Sciences, Semmelweis University, Budapest, Hungary

7        <sup>2</sup>Epilepsy Center, National Institute of Clinical Neurosciences, Budapest, Hungary

8        <sup>3</sup>Institute of Cognitive Neuroscience and Psychology, Research Centre for Natural Sciences, Budapest,  
9        Hungary

10       <sup>4</sup>Department of General Psychology, Pázmány Péter Catholic University, Budapest, Hungary

11       <sup>5</sup>MTA-PPKE Adolescent Development Research Group, Budapest, Hungary

12       <sup>6</sup>Institute of Psychology, ELTE, Eötvös Loránd University, Budapest, Hungary

13       <sup>7</sup>UR2NF, Neuropsychology and Functional Neuroimaging Research Unit at CRCN - Center for  
14       Research in Cognition and Neurosciences and UNI - ULB Neurosciences Institute, Université Libre de  
15       Bruxelles (ULB), Brussels, Belgium

16       <sup>8</sup>Doctoral School of Psychology (Cognitive Science), Budapest University of Technology and  
17       Economics, Budapest, Hungary

18       <sup>9</sup>Max Planck Institute of Psychiatry, Research Group Sleep Endocrinology, Munich, Germany

19       <sup>10</sup>Centre of Mental Health, Klinikum Ingolstadt, Ingolstadt, Germany

20       <sup>11</sup>Donders Institute for Brain, Cognition and Behaviour, Radboud University Medical Center,  
21       Nijmegen, The Netherlands

22

23       **\* Corresponding author**

24       E-mail: [bodizs.robert@med.semmelweis-univ.hu](mailto:bodizs.robert@med.semmelweis-univ.hu)

25       **Short title: Spectral intercepts, slopes and peaks of NREM sleep EEG**

## 26 **Abstract**

27           A novel method for deriving composite, non-redundant measures of non-rapid eye  
28 movement (NREM) sleep electroencephalogram (EEG) is developed on the basis of the  
29 power law scaling of the Fourier spectra. Measures derived are the spectral intercept, the  
30 slope (spectral exponent), as well as the maximal whitened spectral peak amplitude and  
31 frequency in the sleep spindle range. As a proof of concept, we apply these measures on a  
32 large sleep EEG dataset (N = 175; 81 females; age range: 17–60 years) with previously  
33 demonstrated effects of age, sex and intelligence. As predicted, aging is associated with  
34 decreased overall spectral slopes (increased exponents) and whitened spectral peak  
35 amplitudes in the spindle frequency range. In addition, age associates with decreased sleep  
36 spindle spectral peak frequencies in the frontal region. Women were characterized by higher  
37 spectral intercepts and higher spectral peak frequencies in the sleep spindle range. No sex  
38 differences in whitened spectral peak amplitudes of the sleep spindle range were found.  
39 Intelligence correlated positively with whitened spectral peak amplitudes of the spindle  
40 frequency range in women, but not in men. Last, age-related increases in spectral exponents  
41 did not differ in subjects with average and high intelligence. Our findings replicate and  
42 complete previous reports in the literature, indicating that the number of variables describing  
43 NREM sleep EEG can be effectively reduced in order to overcome redundancy and Type I  
44 statistical errors in future electrophysiological studies of sleep.

45 **Keywords:** spectral slope; spectral intercept; spectral peak; EEG; NREM sleep, FFT

46

47

## 48 **Author summary**

49 Given the tight reciprocal relationship between sleep and wakefulness, the objective  
50 description of the complex neural activity patterns characterizing human sleep is of utmost  
51 importance in understanding the several facets of brain function, like sex differences, aging  
52 and cognitive abilities. Current approaches are either exclusively based on visual impressions  
53 expressed in graded levels of sleep depth (W, N1, N2, N3, REM), whereas computerized  
54 quantitative methods provide an almost infinite number of potential metrics, suffering from  
55 significant redundancy and arbitrariness. Our current approach relies on the assumptions that  
56 the spontaneous human brain activity as reflected by the scalp-derived electroencephalogram  
57 (EEG) are characterized by coloured noise-like properties. That is, the contribution of  
58 different frequencies to the power spectrum of the signal are best described by power law  
59 functions with negative exponents. In addition, we assume, that stages N2–N3 are further  
60 characterized by additional non-random (non-noise like, sinusoidal) activity patterns, which  
61 are emerging at specific frequencies, called sleep spindles (9–18 Hz). By relying on these  
62 assumptions we were able to effectively reduce 191 spectral measures to 4: (1) the spectral  
63 intercept reflecting the overall amplitude of the signal, (2) the spectral slope reflecting the  
64 constant ratio of low over high frequency power, (3) the frequency of the maximal sleep  
65 spindle activity and (4) the amplitude of the sleep spindle spectral peak. These 4 measures  
66 were efficient in characterizing known age-effects, sex-differences and cognitive correlates of  
67 sleep EEG. Future clinical and basic studies are supposed to be significantly empowered by  
68 the efficient data reduction provided by our approach.

## 69 Introduction

70 The frequency characteristics of sleep-dependent neuronal oscillations as recorded by  
71 scalp electroencephalography (EEG) are increasingly recognized as potent markers of aging  
72 (Pótári et al., 2017; Ujma et al., 2019), health and disease (Kaskie and Ferrarelli, 2019),  
73 typical and atypical development and maturation (Campbell et al., 2012; Bódizs et al., 2012),  
74 as well as of neurocognitive features of high practical relevance (Bódizs et al., 2005; Ujma et  
75 al., 2017; Ujma, 2018). However, many of these studies are suffering from increased  
76 susceptibility to Type I error as a result of an inherently increased level of “researcher degrees  
77 of freedom”. That is, EEG data can be analysed in almost infinite different ways, by focusing  
78 on one or another specific electrophysiological phenomenon (Ujma, 2018; Ujma et al., 2020).  
79 Instead of focusing on multiple frequencies or phenomena, our aim is to provide an overall  
80 characterization of the broadband NREM sleep EEG. Our data-driven approach is based on  
81 the statistical properties of the signal, in order to assess the intercept and the slope, as well as  
82 the most prominent/important spectral peaks of the Fourier spectrum.

83 Evidence suggests the linear relationship between the logarithmic amplitude or power  
84 of EEG and the logarithm of frequency (Feinberg et al., 1984; Pereda et al., 1998). Such  
85 power law scaling is a general, state-independent feature of cortical EEG, suggesting that the  
86 Fourier spectrum can be reliably described by an approximation of the parameters of the  
87 following function:

$$88 \quad P(f) = Cf^\alpha \quad (1)$$

89 where  $P$  is power ( $P \geq 0$ ) as a function of frequency ( $0 \leq f \leq f_{Nyquist}$ ),  $C$  is the constant (or the  
90 intercept) expressing the overall, frequency-independent EEG amplitude ( $C > 0$ ), whereas  $\alpha$  is  
91 the spectral exponent indicating the decay rate (slope) of power as a function of frequency.  
92 Reported values for the spectral exponent are  $-4 < \alpha < -1$ , with lower values indicating lower

93 arousal/deeper sleep, but the values might depend on the EEG reference used, e.g. bipolar  
94 derivations result in higher  $\alpha$  values as compared to referential ones, as well (Freemen et al.,  
95 2006; Lázár et al., 2020). That is, instead of providing 191 values for the power spectra of  
96 0.5–48 Hz activity in bins of 0.25 Hz, we need just 2 ( $C$  and  $\alpha$ ). Most notably, if reliable, this  
97 function suggests that classical bandwise or binwise spectral analyses are not considering the  
98 frequency-determined nature of power values when applying statistical tests focusing on  
99 specific oscillatory phenomena.

100         However, there are further specific features of the EEG spectrum, known as spectral  
101 peaks, which are upward deflections in the decreasing power law trend described by function  
102 (1) above. These peaks reflect non-random oscillatory activities of specific frequencies, which  
103 might prevent the reliable estimation of  $\alpha$  if they are not considered (Freeman and Zhai, 2009,  
104 Colombo et al., 2019). In order to deliberately describe the power spectrum by taking into  
105 account its prominent peaks, we suggest the inclusion of a peak power function in the formula  
106 as follows:

$$107 \quad P(f) = Cf^\alpha P_{Peak}(f) \quad (2)$$

108 Peak power ( $P_{Peak}$ ) at frequency  $f$  equals 1 if there is no peak and is larger than 1 if there is a  
109 spectral peak at that frequency. Thus, the number of parameters is increased by considering  
110 spectral peaks, but is still lower than the values included in the original spectra, as putative  
111 “no peak regions” can be compressed in series of all ones. It has to be noted, that  $P_{Peak}(f)$  is a  
112 whitened power measure, because it is independent from the spectral slope ( $\alpha$ ), which  
113 constitute the coloured part of the spectrum (Fig 1). In the following we only consider the  
114 maximal peaks, for which  $P_{Peak}(f) \leq P_{Peak}(f_{maxPeak})$ . No multiple peaks are analysed in this  
115 report.

116

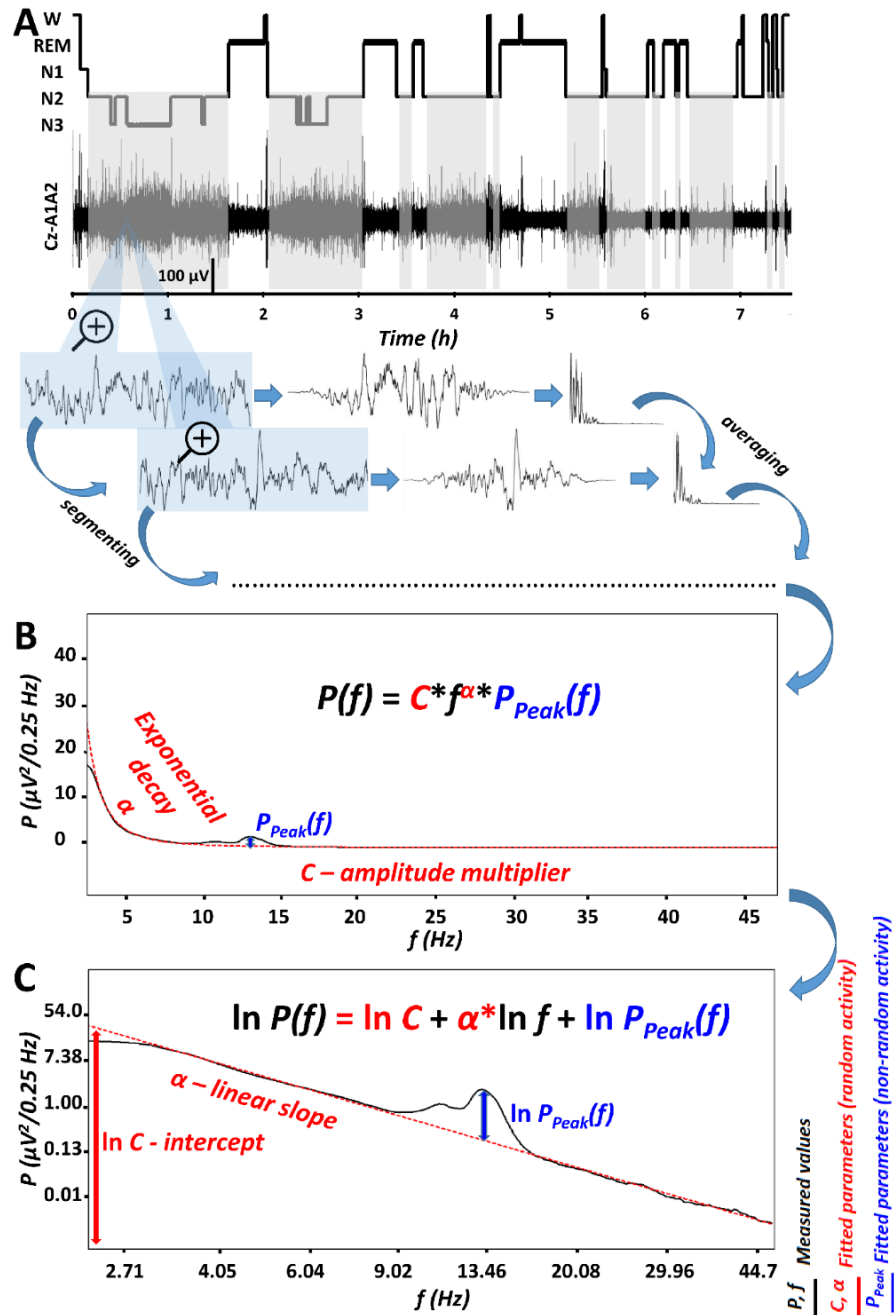
117 *Fig 1. The parametrization of non-*  
 118 *rapid eye movement (NREM) sleep*  
 119 *electroencephalogram (EEG)*  
 120 *spectra. A. Hypnogram and steps of*  
 121 *the spectral EEG analyses as*  
 122 *exemplified in a representative*  
 123 *record of a young male volunteer.*  
 124 *Grey shaded areas represent NREM*  
 125 *sleep, which is analysed in the*  
 126 *present report. Blue-shaded EEG*  
 127 *segments are magnified 4 seconds*  
 128 *long epochs, with 2 seconds overlap*  
 129 *and modified with a Hanning*  
 130 *window before power spectral*  
 131 *analysis via mixed-radix Fast*  
 132 *Fourier Transformation (FFT). B.*  
 133 *Average spectral power (P) is*  
 134 *characterized by a frequency (f)-*  
 135 *dependent exponential decay ( $\alpha$ ), as*  
 136 *well as by an overall, frequency-*  
 137 *independent amplitude multiplier*  
 138 *(C) and a peak power multiplier at*  
 139 *critical frequencies [ $P_{Peak}(f)$ ]. C.*  
 140 *The natural logarithm of spectral*  
 141 *power (P) is a linear function of the*  
 142 *natural logarithm of frequency (f),*  
 143 *characterized by a linear slope  $\alpha$*   
 144 *(which is equal with  $\alpha$  in panel B)*  
 145 *and an intercept (the latter being the*  
 146 *natural logarithm of the amplitude*  
 147 *multiplier, C in panel B). In addition, this linear function has to be summed with the natural*  
 148 *logarithm of the peak power multiplier [ $P_{Peak}(f)$ , equal to the same frequency-dependent*  
 149 *function in panel B]. Please note that “no peak regions” can be compressed in series of all*  
 150 *ones, resulting in reduced number of variables as compared to the bins in the original*  
 151 *spectra.*

152

153

154

155



As a proof of concept, we apply these measures on a large sleep EEG dataset with previously demonstrated effects of individual differences. Specifically, we translate some core findings regarding age, sex, and general intelligence-related effects in NREM sleep EEG into

156 specific hypotheses in terms of  $C$ ,  $\alpha$ , and two indexes of spindle-range  $P_{Peak}(f)$ : whitened  
157 spectral peak amplitude  $P_{Peak}(f_{maxPeak})$  and spectral peak frequency ( $f_{maxPeak}$ ).

158 Age was reported to correlate negatively with NREM sleep EEG slow wave activity,  
159 but positively with high frequency activity in healthy adult subjects (Carrier et al., 2001). An  
160 early study based on period amplitude analysis reported that NREM sleep EEG log amplitude  
161 is a linear function of log frequency and that the slope of this linear decay is steeper in young  
162 as compared to older adults (Feinberg et al., 1984). Thus, we hypothesize (H1) that the slope  
163 of the Fast Fourier Transformation (FFT)-based spectrum of NREM sleep EEG ( $\alpha$ ) is age-  
164 dependently increasing (less steep decreasing trends are indexed by higher exponents  $\alpha$ ). In  
165 addition, aging was shown to be associated with decreased sleep spindle activity (Nicolas et  
166 al., 2001; Purcell et al., 2017), thus we hypothesize (H2) a negative correlation between age  
167 and  $P_{Peak}(f_{maxPeak})$  values characterizing maximal spindle frequency spectral peaks ( $9 \text{ Hz} < f <$   
168  $18 \text{ Hz}$ ). In addition to decreased spindle activity, the increase in intra-spindle oscillatory  
169 frequency (Hz) was shown to be a characteristic feature of aging according to some (Principe  
170 and Smith, 1982; Nicolas et al., 2001), but not all (Purcell et al., 2017) reports. As a  
171 consequence, we hypothesize (H3) that the maxima of the  $P_{Peak}(f)$  function for  $9 \text{ Hz} < f < 18$   
172  $\text{Hz}$  (broad spindle range) emerge at higher  $f_{maxPeak}$  values in aged, as compared to young  
173 subjects.

174 Reported sex differences in NREM and REM sleep EEG indicate higher spectral  
175 power in several frequency bands in women, as compared to men (Dijk et al., 1989; Carrier et  
176 al., 2001). Such broad band and state-independent differences suggest a general tendency for  
177 a higher EEG amplitude in women, due to non-neuronal factors, like skull thickness and bone  
178 mineral density (Dijk et al., 1989; Looker et al., 2009). As a consequence, we hypothesize  
179 (H4) that women are characterized by higher spectral intercepts, than men ( $C_{\text{♀}} > C_{\text{♂}}$ ). As a  
180 consequence of this point we will reanalyze some of the reported sex differences in sleep



181 spindle density/power, indicating increased sleep spindling in women as compared to men  
182 (Dijk et al., 1989; Carrier et al., 2001; Crowley, 2002; Huupponen et al., 2002), by relying on  
183 whitened spectral peak amplitudes of the spindle range ( $P_{Peak}(f_{maxPeak})$ ).

184 Another sex difference was reported in terms of sleep spindle frequency, that is  
185 women were shown to be characterized by higher oscillatory frequencies as compared to men  
186 (Ujma et al., 2014). We hypothesize (H5) that 9–18 Hz  $P_{Peak}(f)$  maxima occurs at higher  $f$   
187 values in women as compared to men ( $f_{maxPeak♀} > f_{maxPeak♂}$ ).

188 Intelligence was shown to correlate positively with NREM sleep EEG sleep spindle  
189 activity (Bódizs et al., 2005). Although, a recent metaanalysis casts doubt on the sexual  
190 dimorphism of this relationship (Ujma, 2018), the dataset we analyse in our current report is  
191 characterized by a clear difference among women and men: women were characterized by  
192 positive correlation between sleep spindle amplitude/power and IQ, whereas null correlations  
193 were reported for men (Ujma et al., 2014; Ujma et al., 2017). As our current analyses are  
194 based on the same dataset, we hypothesize (H6) that  $P_{Peak}(f_{maxPeak})$  values of the sleep spindle  
195 range (9–18 Hz) correlate positively with IQ in women, but not in men. Intelligence was also  
196 reported to modulate the relationship between the decrease in NREM sleep EEG slow activity  
197 associated with aging: participants showing average IQ (AIQ) scores were characterized by  
198 significant negative correlations regarding age vs. slow wave activity, whereas no such  
199 correlations were found in individuals with high IQ (HIQ) (Pótári et al., 2017). As the original  
200 report provided overwhelming evidence for an age vs relative delta power correlation as being  
201 modulated by IQ range, whereas weaker evidence was found for absolute power (Pótári et al.,  
202 2017), we do not know if this finding reflects the age-dependency of slow wave activity per  
203 se, or the combined age-dependency of slow wave activity and slow/high activity ratio. The  
204 former scenario would fit with a null effect for IQ-modulation of age vs spectral slope



205 correlation, whereas the latter would lead to an IQ-dependence of age vs spectral slope  
206 relationship (H7).

207

## 208 **Results**

### 209 **Goodness of fit: Is the logarithm of spectral power a linear function of the logarithm of** 210 **frequency?**

211         Linears were fitted to the equidistant log-log plots of the EEG power spectra in the 2–  
212 48 Hz range, excluding the 6–18 Hz range, the latter known to be characterized by spectral  
213 peaks in NREM sleep (Fig. 1C, see details in section Methods). The sample mean of fitted  
214 slopes ( $\bar{\alpha}$ ) varied between -2.73 (SD = 0.22) and -2.33 (SD = 0.22) for the frontocentral (Fz)  
215 and left posterior temporal (T5) region, respectively. In turn, the sample mean of the  
216 intercepts ( $\overline{\ln C}$ ) varied between 3.74 (SD = 0.73) and 5.76 (SD = 0.69) for derivations T5  
217 and Fz, respectively. Goodness of fit ( $R^2$ ) of the linear model of the equidistant 2–6 Hz and  
218 18–48 Hz spectral data varied in the range of 0.8955–0.9997 across subjects and EEG  
219 derivations. The square of the Fisher Z-transformed, averaged and back-transformed Pearson  
220 correlations between the fitted linear and the spectral data is  $\overline{R^2} = 0.9952$  (SD = 0.1578).

221

### 222 **H1: Age-associated increase in the spectral exponent (decrease in spectral slope) of** 223 **NREM sleep EEG**

224         Spearman rank correlations ( $\rho$ ) indicated a significant positive association between age  
225 (years) and NREM sleep EEG spectral exponents ( $\alpha$ ) at all derivations (Table 1a). The  
226 Rüger's area including all derivations proved to be significant at both of the new critical

227 probability ( $p$ ) levels (0.025 and 0.017). Thus, based on the Descriptive Data Analysis (DDA,  
 228 see details in section Methods) procedure (Abt, 1987; Abt, 1990), this area can be considered  
 229 as a significant one (see also Fig 2A).

230

231 *Table 1. Spearman rank correlations between age and spectral exponents, as well as spectral*  
 232 *peak amplitudes and frequencies in the sleep spindle range of NREM sleep EEG*

Deriva- tion	a, slope ( $\alpha$ )			b, peak amplitude ( $P_{Peak}(f_{maxPeak})$ )			c, peak frequency ( $f_{maxPeak}$ )		
	N	Spearman's $\rho$	p	N	Spearman's $\rho$	p	N	Spearman's $\rho$	p
Fp1	163	.382	<.001***	150	-.107	.193	150	-.222	.006***
Fp2	171	.392	<.001***	155	-.035	.669	155	-.215	.007***
F3	174	.396	<.001***	166	-.184	.018**	166	-.279	<.001***
F4	173	.427	<.001***	165	-.17	.029*	165	-.258	.001***
Fz	156	.447	<.001***	151	-.288	<.001***	151	-.378	<.001***
F7	153	.362	<.001***	137	-.105	.223	137	-.292	.001***
F8	154	.386	<.001***	141	-.002	.978	141	-.217	.010***
C3	174	.38	<.001***	172	-.328	<.001***	172	-.057	.46
C4	175	.395	<.001***	172	-.32	<.001***	172	-.042	.586
Cz	156	.357	<.001***	155	-.409	<.001***	155	-.063	.44
P3	175	.348	<.001***	175	-.23	.002***	175	.107	.16
P4	175	.378	<.001***	174	-.227	.003***	174	.087	.253
T3	154	.395	<.001***	125	-.141	.116	125	-.14	.119
T4	156	.394	<.001***	131	-.125	.154	131	-.3	.001***
T5	154	.337	<.001***	152	-.176	.030*	152	.014	.861
T6	155	.377	<.001***	151	-.213	.009***	151	-.001	.988
O1	175	.295	<.001***	173	-.127	.097	173	.103	.179
O2	174	.331	<.001***	172	-.132	.085	172	.11	.152

233 \*  $p < .05$ ; \*\*  $p < .025$ ; \*\*\*  $p < .017$

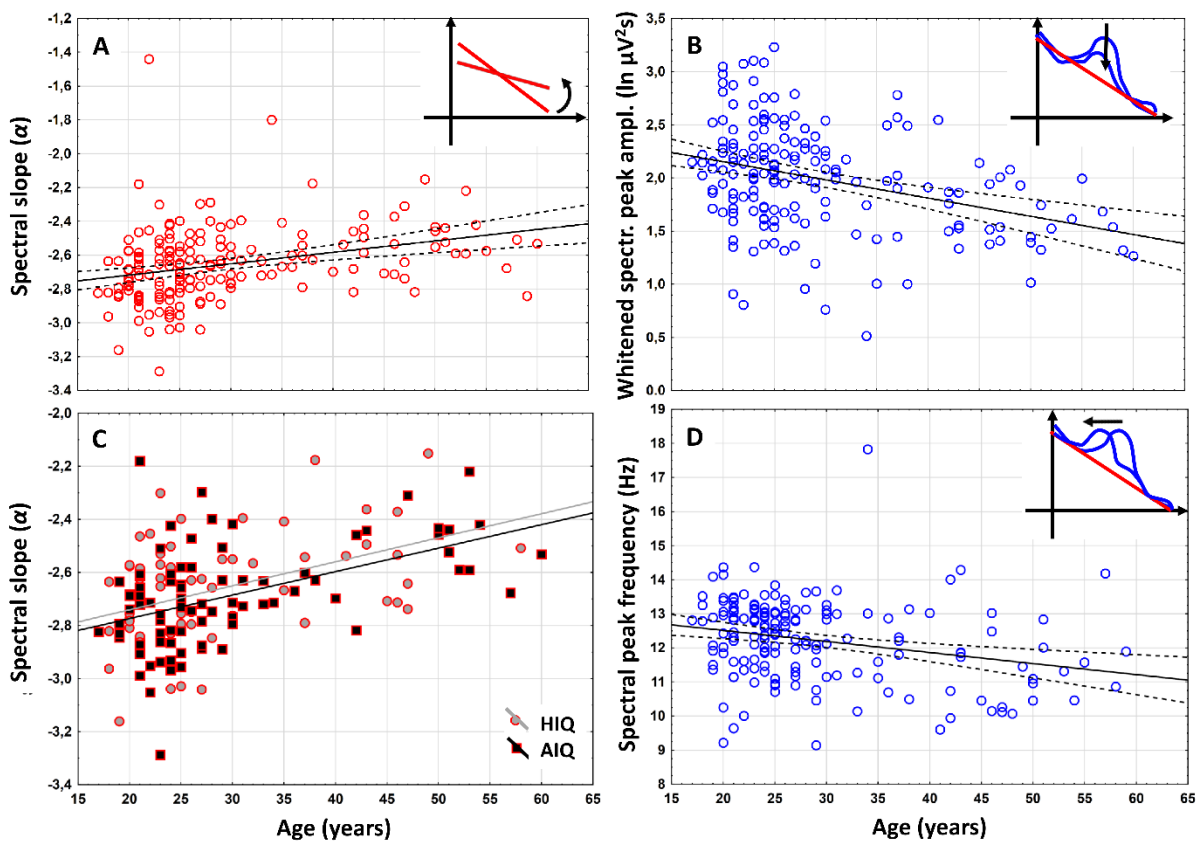
234 *a, Correlation between age and spectral exponents ( $\alpha$ ) of NREM sleep EEG. Note the*  
 235 *significance of all correlations at the descriptive level of significance ( $p < .05$ ), as well as at*  
 236 *both of the new critical  $p$  levels corresponding to  $p < .025$  and  $p < .017$ . The minimum criteria*  
 237 *of a significant Ruger's area is 10 out of 18 descriptive significances to meet the  $p < .025$  and*  
 238 *7 out of 18 descriptive significances to meet the  $p < .017$  criteria.*

239 *b, Correlations between age and whitened maximal spectral peak amplitude  $P_{Peak}(f_{maxPeak})$  of*  
 240 *NREM sleep EEG spindle frequency activity (9 Hz <  $f$  < 18 Hz). Note the descriptive*  
 241 *significance of 9 correlations forming a large Ruger area in the bilateral fronto-centro-parietal*  
 242 *and posterior temporal region. The minimum criteria for a significant Ruger area is at least 5*  
 243 *correlations to be significant at  $p < .025$  and 4 at  $p < .017$ . Here we found 5 and 4 correlations*

244 meeting this criteria, respectively. Thus, the Ruger area can be considered as a global zone of  
245 significance.

246 c, Correlations between age and NREM sleep EEG maximal spectral peak frequencies in the  
247 spindle range ( $f_{maxPeak}$ ). Note the descriptive significance of 8 negative correlations forming a  
248 Ruger area in the bilateral frontal and right temporal region. The minimum criteria for a  
249 significant Ruger area is at least 5 correlations to be significant at  $p < .025$  and 3 at  $p < .017$ .  
250 Here we found 8 for both, thus, the Ruger area can be considered as a global zone of  
251 significance.

252



253

254 Fig 2. Representative scatterplots of the correlations between age and measures of the NREM  
255 sleep EEG spectra at derivation F3. A. Correlation of age with the spectral exponent ( $\alpha$ )  
256 indicating a decrease in the spectral slope in the aged subjects. B. Correlations of age with  
257 the whitened maximal spectral peak amplitude in the sleep spindle frequency range  
258 ( $P_{Peak}(f_{maxPeak})$ ). Note the decrease in whitened spectral peak amplitude in the aged. C.  
259 Correlation of age with the NREM sleep EEG spectral exponent ( $\alpha$ ) as categorized by  
260 intelligence (HIQ – High Intelligence Quotient, AIQ – Average Intelligence Quotient). Note  
261 the lack of an IQ effect. D. Correlation of age with NREM sleep EEG maximal spectral peak  
262 frequency ( $f_{maxPeak}$ ) in the spindle range. Note the age-dependent decline in frequency. Color  
263 codes are consistent with Fig 1: red – spectral slopes, blue – spectral peaks.

264

265 **H2: Age-dependent decrease in whitened spectral peak amplitude of NREM sleep EEG**  
266 **sleep spindle frequencies**

267 Based on Spearman's rank correlations ( $\rho$ ), maximal whitened spectral peak amplitudes  
268 of NREM sleep EEG spindle frequencies ( $P_{Peak}(f_{maxPeak})$ ) and age correlated negatively at 10  
269 derivations covering the frontocentral, parietal and posterior temporal areas (F3, F4, Fz, C3,  
270 Cz, C4, T5, T6, P3, and P4). Among these 10 derivations defining the Ruger area based on  
271 descriptive significances, 8 were significant at  $p < .025$  and 7 at  $p < .017$  (Table 1b). That is the  
272 Ruger area indicates a negative correlation between age and whitened sleep spindle spectral  
273 peak amplitude (see a representative example in Fig 2B).

274

275 **H3: Age-related decrease but not increase in spectral peak frequency of NREM sleep**  
276 **EEG spindle range activity was found**

277 Based on Spearman's rank correlation ( $\rho$ ) maximal sleep spindle spectral peak emerge  
278 at lower  $f_{maxPeak}$  values in the frontal region of aged, as compared to young subjects. This  
279 finding evidently contrasts our prediction. Peak frequency and age correlated negatively at 8  
280 derivations covering the frontal and the right temporal areas (Fp1, Fp2, F3, F4, Fz, F7, F8 and  
281 T4). This Ruger's area was significant, as all correlations conformed to both of the new  
282 critical probabilities (Table 1c, Fig 3D).

283

284 **H4: NREM sleep EEG spectral intercepts, but not whitened spindle spectral peak**  
285 **amplitudes are higher in women as compared to men**

286 Mann-Whitney U test revealed that women are characterized by significantly higher  
287 spectral intercepts (the natural logarithm of  $C$  values in formula (1) and (2)) compared to men

288 at all derivations. After correction for multiple testing the Ruger-area remained significant  
 289 (Table 2). As predicted women and men did not differ in NREM sleep EEG maximal spectral  
 290 peak amplitudes of the spindle range ( $P_{Peak}(f_{maxPeak})$ ) at any of the derivations (Table 2b).

291

292 *Table 2. Women vs men differences in NREM sleep EEG spectral intercepts and whitened*  
 293 *peak amplitudes in the spindle range*

	a, intercept (ln C)						b, peak amplitude ( $P_{Peak}(f_{maxPeak})$ )					
	U	p	N♀	Md♀	N♂	Md♂	t	p	N♀	$\bar{x}_{\text{♀}}$	N♂	$\bar{x}_{\text{♂}}$
Fp1	2455	.004***	77	5.11	86	4.84	-.098	.924	67	1.370	83	1.379
Fp2	2682	.003***	81	5.14	90	4.87	.515	.619	68	1.404	87	1.361
F3	2658	.001***	81	5.53	93	5.22	.420	.675	75	1.731	91	1.699
F4	2503	<.001***	81	5.58	92	5.28	1.003	.317	76	1.760	89	1.684
Fz	1997	.001***	69	6.04	87	5.61	.836	.405	66	1.804	85	1.736
F7	2295	.031*	67	4.58	86	4.28	1.474	.162	59	1.470	78	1.336
F8	2382	.046*	69	4.56	85	4.44	.710	.493	63	1.388	78	1.327
C3	2345	<.001***	81	5.36	93	4.98	-.059	.953	80	1.989	92	1.994
C4	2483	<.001***	81	5.41	94	5.04	.225	.822	79	1.983	93	1.966
Cz	1869	<.001***	69	5.98	87	5.58	.434	.665	68	2.145	87	2.108
P3	2467	<.001***	81	4.97	94	4.69	-.397	.692	81	2.241	94	2.274
P4	2423	<.001***	81	5.04	94	4.56	-.704	.483	81	2.144	93	2.202
T3	2270	.019**	67	3.99	87	3.72	1.028	.306	55	1.254	70	1.169
T4	2428	.041*	69	4.02	87	3.83	.984	.327	57	1.197	74	1.119
T5	2172	.006***	68	3.92	86	3.67	-1.095	.275	68	1.545	84	1.631
T6	2021	.001***	68	3.91	87	3.65	-.460	.646	66	1.475	85	1.509
O1	2182	<.001***	81	4.51	94	3.97	-1.072	.285	80	1.692	93	1.783
O2	2102	<.001***	81	4.53	93	4.04	-1.938	.054	80	1.592	92	1.748

294 *a. Mann-Whitney U tests indicate higher spectral intercepts (ln C values) in the female (♀) as*  
 295 *compared to the male (♂) subgroup. Descriptive significance was observed at all (18)*  
 296 *recording locations. Minimum criteria of a significant Ruger area requires at least 10 of*  
 297 *these p values to be lower than .025 and 7 of them to be less than .017. Observed values are*  
 298 *15 and 14, respectively. Thus, the Ruger area characterizing the sex differences in NREM*  
 299 *sleep EEG spectral intercepts is significant. Md – median; \*  $p < .05$ ; \*\*  $p < .025$ ; \*\*\*  $p <$*   
 300 *.017.*

301 *b. Whitened maximal spectral peak amplitudes in the sleep spindle range of NREM sleep EEG*  
 302 *( $P_{Peak}(f_{maxPeak})$ ) do not significantly differ between females and males.*

303

304 **H5: Women are characterized by higher NREM sleep EEG spectral peak frequencies in**  
 305 **the spindle range**

306 According to Mann-Whitney U Tests, women were characterized by significantly  
 307 higher  $f_{maxPeak}$  values as compared to men, except derivations T3 and T4. The area remained  
 308 significant after the correction for multiple testing (Table 3).

309

310 *Table 3. Women vs men differences in NREM sleep EEG spindle spectral peak frequencies*

	U	p	N♀	Md♀	N♂	Md♂
Fp1	1888	.001***	67	11.97	83	11.32
Fp2	1864	.000***	68	12.00	87	11.29
F3	2191	.000***	75	12.80	91	11.86
F4	2217	.000***	76	12.98	89	11.80
Fz	2259	.041*	66	13.06	85	12.51
F7	1492	.000***	59	12.23	78	11.59
F8	1608	.000***	63	12.14	78	11.49
C3	2651	.002***	80	13.53	92	13.26
C4	2502	.000***	79	13.60	93	13.28
Cz	1830	.000***	68	13.68	87	13.33
P3	2290	.000***	81	13.71	94	13.36
P4	2368	.000***	81	13.70	93	13.38
T3	1829	.635	55	12.80	70	12.91
T4	1942	.440	57	12.94	74	12.93
T5	1893	.000***	68	13.62	84	13.32
T6	1730	.000***	66	13.63	85	13.33
O1	2282	.000***	80	13.65	93	13.33
O2	2253	.000***	80	13.65	92	13.35

311 *Mann-Whitney U test indicates that women as compared to men are characterized by higher*  
 312  *$f_{maxPeak}$  values at which spindle range  $P_{Peak}(f)$  maxima emerge. The Rüger area contains 16*  
 313 *nominally significant effects. 15 of these women vs men differences were significant at both of*  
 314 *the more stringent criteria ( $p < .025$  and  $p < .017$ ), which supports the significance of the*  
 315 *area. Md – median; \*  $p < .05$ ; \*\*  $p < .025$ ; \*\*\*  $p < .017$ .*

316

317

318 **H6: IQ correlates positively with NREM sleep EEG spindle range whitened spectral**  
 319 **peak amplitude in women**

320 Pearson correlations revealed significant associations of whitened maximal spectral  
 321 peak amplitudes ( $P_{Peak}(f_{maxPeak})$ ) pertaining to NREM sleep EEG spindle activity with IQ at  
 322 derivations C3 (N = 67,  $r = .33$ ,  $p = .007$ ), C4 (N = 66,  $r = .34$ ,  $p = .005$ ), Cz (N = 55,  $r = .34$ ,  
 323  $p = .010$ ), P3 (N = 68,  $r = .26$ ,  $p = .031$ ), P4 (N = 68,  $r = .28$ ,  $p = .020$ ), and T3 (N = 45,  $r =$   
 324  $.32$ ,  $p = .031$ ) in women (Table 4; Fig 3). The R<sub>üger</sub> area at this centroparietal-left temporal  
 325 region remained significant after the control for multiple testing (4/6 correlations are  
 326 significant at .05/2 and 3/6 correlations at .05/3). No significant correlations of whitened  
 327 spectral peak amplitude and IQ were found in men.

328

329 *Table 4. Correlation of whitened spectral peak amplitudes with IQ in women and men*

Derivation	$r_{\text{♀}}$	$p_{\text{♀}}$	$N_{\text{♀}}$	$r_{\text{♂}}$	$p_{\text{♂}}$	$N_{\text{♂}}$
Fp1	.24	.067	55	.02	.830	72
Fp2	.16	.231	55	.01	.985	77
F3	.15	.216	62	-.01	.920	78
F4	.17	.178	63	-.01	.989	76
Fz	.22	.101	53	.08	.499	72
F7	.11	.432	48	.02	.858	67
F8	.02	.880	52	.03	.759	66
C3	.32	.006***	67	.02	.842	79
C4	.34	.004***	66	.03	.746	81
Cz	.34	.010***	55	.09	.426	74
P3	.26	.030*	68	-.07	.531	81
P4	.28	.020**	68	-.05	.627	81
T3	.32	.030*	45	.09	.484	58
T4	.23	.118	46	-.04	.718	62
T5	.19	.147	55	.03	.771	72
T6	.15	.266	54	.06	.609	73
O1	.22	.061	67	.03	.731	81
O2	.23	.057	67	.01	.888	80

330 *The R<sub>üger</sub> area at the centroparietal-left temporal region characterized by descriptive*  
 331 *significances ( $p < .05$ ) in the female subgroup (♀) remained significant after the control for*  
 332 *multiple testing (4/6 correlations are significant at .05/2 and 3/6 at .05/3). No significant*



333 correlations of whitened spectral peak amplitude and IQ were found in the male subgroup  
 334 ( $\sigma$ ). \*  $p < .05$ ; \*\*  $p < .025$ ; \*\*\*  $p < .017$ .

335

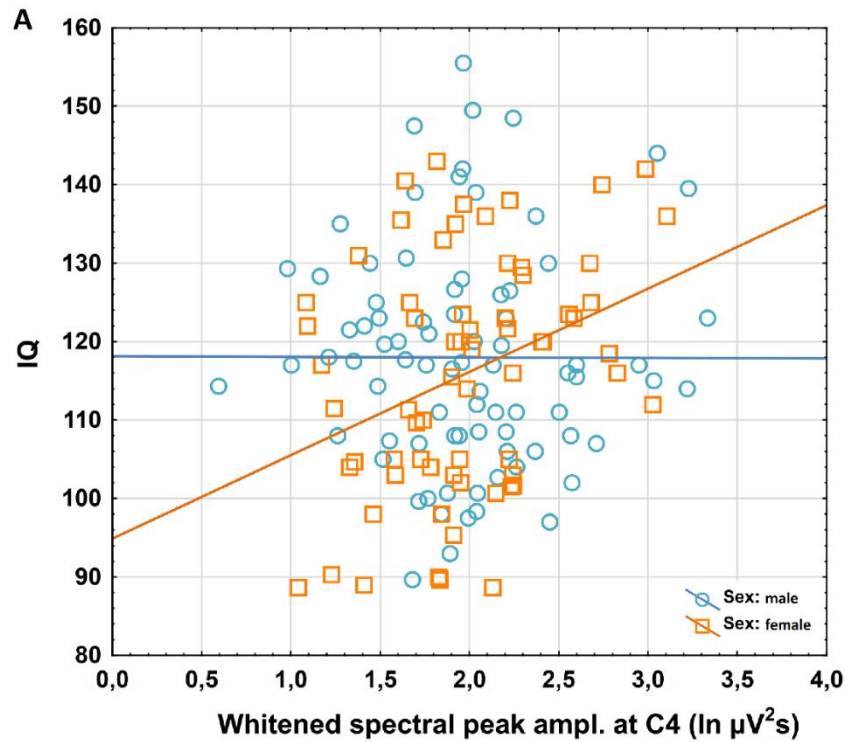
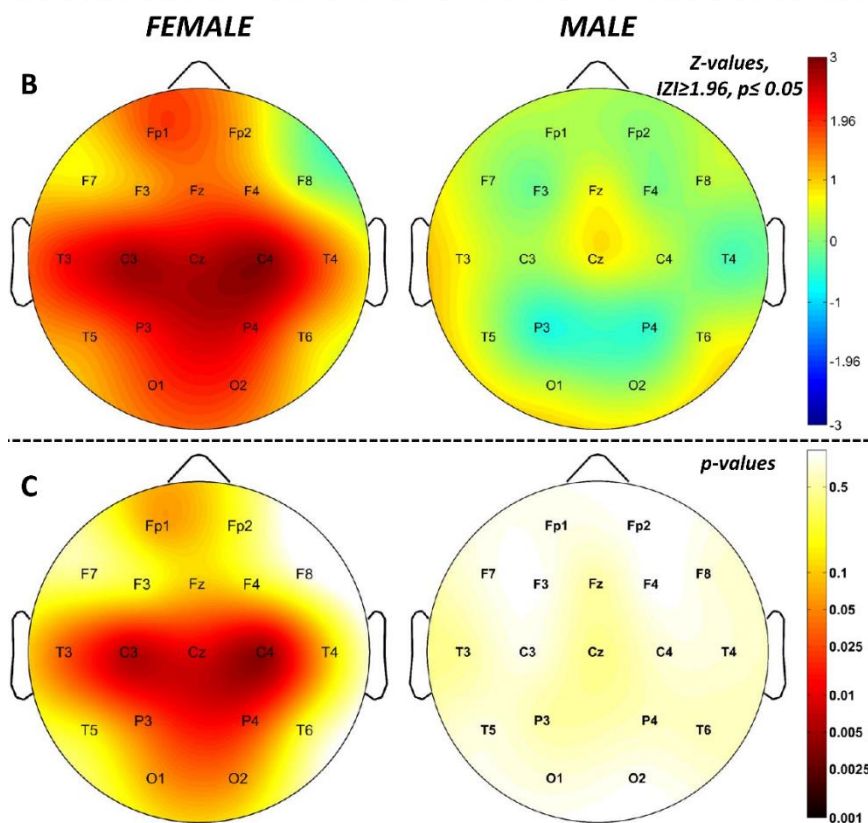


Fig 3. Correlations between NREM sleep EEG spindle frequency whitened spectral peak amplitudes and IQ in females and males. A. Categorized scatterplot representing the correlation between whitened spectral peak amplitude of the NREM sleep EEG spindle frequency range (recording site: F4) and IQ in women and men. B. Pearson  $r$ -values were transformed to  $Z$ -values and represented on topographical maps. C. Significance probability maps of the correlations presented in B.



365 **H7: Do age-related declines in NREM sleep EEG spectral slopes differ among subjects**  
 366 **with average and high IQ?**

367 As already presented in the former subheadings (H1) an age-associated increase in  
 368 spectral exponents (less steep spectral slopes) characterizes the NREM sleep EEG of adult  
 369 volunteers. This effect was separately assessed in subjects with average and high IQ, and  
 370 results were compared. Age and slopes of the NREM sleep EEG spectra ( $\alpha$ ) were significantly  
 371 associated in both subgroups (AIQ and HIQ). We found no significant difference between  
 372 these correlations, however (Table 5). That is, age-associated decreases in the steepness of the  
 373 slopes of the NREM sleep EEG spectra are independent of the subjects' IQ.

374

375 *Table 5. Comparison of the correlations between age and the slope of the NREM sleep EEG*  
 376 *spectrum in subjects with average and high intelligence (AIQ vs HIQ)*

	Spearman's $\rho_{AIQ}$	$N_{AIQ}$	$\rho_{AIQ}$	Spearman's $\rho_{HIQ}$	$N_{HIQ}$	$\rho_{HIQ}$	$p_{\text{difference}}$
Fp1	.44	79	<.001***	.40	60	.001***	.787
Fp2	.44	85	<.001***	.45	63	<.001***	.901
F3	.48	84	<.001***	.41	64	.001***	.622
F4	.52	83	<.001***	.42	64	.001***	.476
Fz	.57	70	<.001***	.45	60	<.001***	.370
F7	.39	70	.001***	.45	58	<.001***	.660
F8	.45	69	<.001***	.43	59	.001***	.900
C3	.44	84	<.001***	.45	64	<.001***	.956
C4	.45	85	<.001***	.43	64	<.001***	.896
Cz	.47	70	<.001***	.37	60	.004***	.507
P3	.39	85	<.001***	.42	64	.001***	.801
P4	.42	85	<.001***	.41	64	.001***	.927
T3	.43	70	<.001***	.49	59	<.001***	.640
T4	.51	70	<.001***	.42	60	.001***	.507
T5	.32	70	.007***	.45	58	<.001***	.412
T6	.40	70	.001***	.42	60	.001***	.896
O1	.31	85	.004***	.40	64	.001***	.549
O2	.34	84	.002***	.41	64	.001***	.610

377 *Correlations were significant in both intelligence groups, however, the differences between*  
 378 *the higher (HIQ) and average (AIQ) intelligence groups was not significant ( $p_{\text{difference}}$ ).*

379 *The table contains correlation coefficients (Spearman's  $R$ ), sample sizes ( $N$ ) and the values of*  
380 *significance ( $p$ ) in both groups. \*\*\* $p < .017$*

381

## 382 **Overcoming model redundancy by determining the alternative intercept of the spectra**

383         Although our model resulted in good fit with empirical data in terms of random (non-  
384 oscillatory) activity or coloured noise and the majority of our hypotheses (including the ones  
385 regarding peak power features) were supported by parameters derived from equation (2), the  
386 spectral slope and the intercept are far from being independent in statistical terms. That is,  
387 although women vs men differences emerged in our spectral intercepts ( $\ln C_{\phi} > \ln C_{\delta}$ ) as  
388 predicted in H4 (see Table 2), and no sex differences in NREM sleep EEG spectral slopes ( $\alpha$ )  
389 were observed (Table 6a), the intercepts and the slopes are negatively correlated in our  
390 database (Table 6b): subjects with steeper spectral slopes (lower  $\alpha$  exponents) are  
391 characterized by higher intercepts (apparently higher EEG amplitudes). This might reflect the  
392 position of the intercept, which is at  $\ln f = 0$  ( $f = 1$  Hz). The interpolated 1 Hz power (based on  
393 the fitted line in the double logarithmic plots) partially reflects the steepness of the slope of  
394 the spectrum.

395         In order to overcome the above issue of parameter-interdependency, we derived  
396 alternative intercepts with the aim of determining parts of the interpolated coloured spectrum  
397 at which our parameter do not reflects the steepness of the slope ( $\alpha$ ). We based our search for  
398 this alternative intercept on two assumptions: (1) the alternative (“slope-free”) intercept is  
399 situated at the border of low and high frequency activities, delineated by the reported sleep  
400 deprivation-induced increases and decreases of spectral power, respectively; (2) intercepts  
401 below the border mentioned in point 1. correlate negatively with the spectral slopes, whereas  
402 intercepts above this border correlate positively with slopes. Extended wakefulness of human

403 *Table 6. Data on the lack of sex differences in spectral slopes and the relationship between*  
 404 *spectral slopes and intercepts*

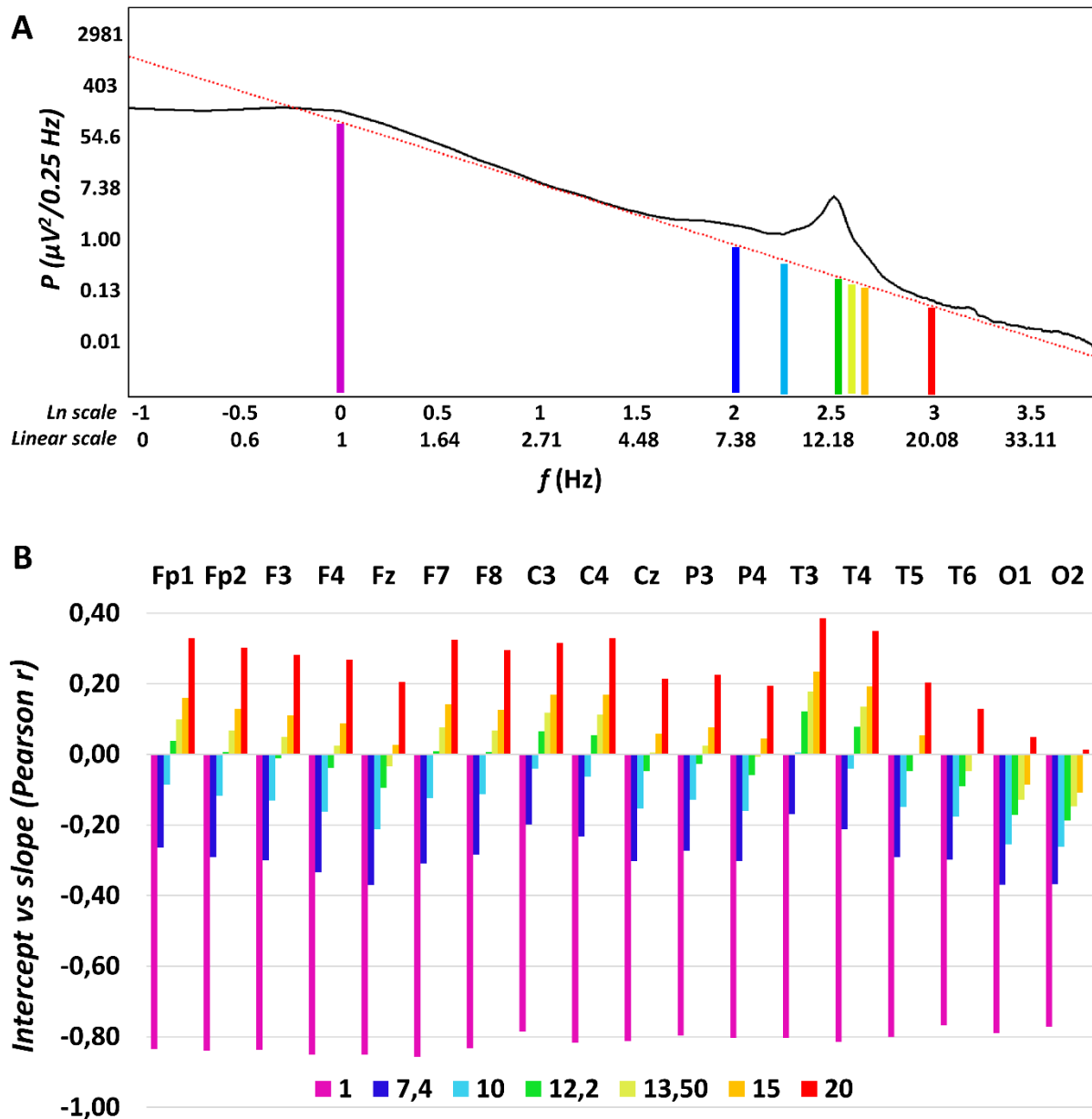
	a, sex differences in $\alpha$						b, $\alpha$ vs $\ln C_0$		
	t	p	$N_{\text{♀}}$	$\overline{\alpha_{\text{♀}}}$	$N_{\text{♂}}$	$\overline{\alpha_{\text{♂}}}$	r	p	N
Fp1	1.452	.148	77	-2.613	86	-2.563	-.83	<.001***	163
Fp2	1.477	.141	81	-2.624	90	-2.575	-.84	<.001***	171
F3	1.578	.116	81	-2.682	93	-2.629	-.83	<.001***	174
F4	1.585	.114	81	-2.689	92	-2.634	-.85	<.001***	173
Fz	1.308	.192	69	-2.760	87	-2.713	-.85	<.001***	156
F7	1.307	.192	67	-2.510	86	-2.460	-.85	<.001***	153
F8	1.276	.203	69	-2.512	85	-2.465	-.83	<.001***	154
C3	2.044	.042*	81	-2.658	93	-2.594	-.78	<.001***	174
C4	1.558	.120	81	-2.664	94	-2.612	-.81	<.001***	175
Cz	.878	.381	69	-2.701	87	-2.672	-.81	<.001***	156
P3	1.407	.161	81	-2.558	94	-2.516	-.79	<.001***	175
P4	1.398	.163	81	-2.553	94	-2.510	-.80	<.001***	175
T3	1.112	.267	67	-2.404	87	-2.362	-.80	<.001***	154
T4	1.031	.303	69	-2.400	87	-2.361	-.81	<.001***	156
T5	.951	.343	68	-2.352	86	-2.317	-.80	<.001***	154
T6	1.358	.176	68	-2.359	87	-2.312	-.76	<.001***	155
O1	1.991	.048*	81	-2.425	94	-2.362	-.79	<.001***	175
O2	2.038	.043*	81	-2.430	93	-2.369	-.77	<.001***	174

405 *a. Sex differences in NREM sleep EEG spectral slopes as revealed by independent sample t-*  
 406 *tests. The 3 descriptive significances do not survive the control of Type I error. b. The*  
 407 *correlation of NREM sleep EEG spectral slopes ( $\alpha$ ) and intercepts at  $\ln f = 0$  ( $\ln C_0$ ).*  
 408 *Correlations are significant over the whole registered area and survive the control of multiple*  
 409 *testing. Fisher z-transformed, averaged and back-transformed correlation value is -0.811.*

410

411 adults is known to increase the NREM sleep EEG spectral power below the sleep spindle  
 412 frequencies, that is the power of 1–9, 1–12 or 1–13 Hz according to different studies (Borbély  
 413 et al., 1981; Finelli et al., 2001; Tinguely et al., 2006; Olbrich et al., 2014; Tarokh et al.,  
 414 2015), whereas power above 10 or 13 Hz was shown to be decreased during recovery sleep  
 415 (Finelli et al., 2001; Tinguely et al., 2006; Tarokh et al., 2015). Thus, we used our fitted  
 416 model parameters  $\alpha$  and  $\ln C$  to determine the interpolated coloured power at frequencies of  
 417 7.4, 10, 12.2, 13.5, 15 and 20 Hz corresponding to natural logarithm values of 2, 2.3, 2.5, 2.6,

418 2.7, and 3, respectively. These alternative intercepts were tested for their independence from  
 419 the slopes ( $\alpha$ ) by Pearson correlations (Fig 4). The pattern of correlations supported our



420

421 *Fig 4. Determining the optimal alternative intercept for the NREM sleep EEG spectra. A.*  
 422 *Linear fitted to the double logarithmic plot of an average NREM sleep EEG spectral power*  
 423 *( $P$ ) derived from right frontopolar location (Fp2) in a young female volunteer. Beside the*  
 424 *original, violet-colored intercept at  $\ln f = 0$  ( $f = 1$  Hz), alternative intercepts are depicted at*  
 425 *7.4, 10, 12.2, 13.5, 15 and 20 Hz. B. Between-subject correlations of the potential intercepts*  
 426 *( $\ln C$ ) with the slopes of the spectra ( $\alpha$ ) in a location-dependent manner. Note the negative*  
 427 *correlations for low and the positive correlation for high frequencies, respectively. Zero-*

428 *correlations are seen in the middle of the sleep spindle frequency range (at 12.2 and 13.5 Hz),*  
429 *although occipital derivations are characterized by a slightly different pattern.*

430

431 assumptions: alternative intercepts below 12.2 Hz were found to correlate negatively with  
432 spectral slopes, whereas above 12.2 or 13.5 Hz (depending on electrode location) positive  
433 correlations were found. That is the best “slope-free” intercepts in the coloured part of the  
434 parametrized NREM sleep EEG spectra are emerging at 12.2 Hz and the 13.5 Hz for anterior  
435 and posterior derivations, respectively ( $\ln C_{2.5}$  and  $\ln C_{2.6}$ ). The original intercept derived at  $\ln$   
436  $f = 0$  could be termed as  $\ln C_0$ , according to this terminology. We reanalyzed H4 in terms of  $\ln$   
437  $C_{2.5}$  and  $\ln C_{2.6}$ . The analyses resulted in increased mean effects sizes from  $\overline{\eta^2} = 0.084$  to  
438  $\overline{\eta^2} = 0.118$  (both averaged over recording locations).

439

## 440 **Discussion**

441 When analyzing the Fourier spectra of EEG records performed for long periods of  
442 sleep, researchers and clinicians rely on statistics. That is, the periodograms of short modified  
443 EEG segments are averaged in order to obtain the averaged spectra (Welch, 1967). As a  
444 consequence, the spectral profiles are inherently statistical in nature. The set of measures  
445 building up this statistical product conform to the power law functions characterized by  
446 negative exponents (Pereda et al., 1998; Freeman and Zhai, 2009), mixed up with a few  
447 positive deflections corresponding to non-random, oscillatory activity patterns (Lázár et al.,  
448 2020). In our view, the characterization of the Fourier spectrum by taking into account its  
449 electrophysiological and statistical regularities might result in an integrated characterization  
450 of NREM sleep EEG, which is superior in terms of construct validity and accuracy. First of  
451 all, a frequency-independent amplitude measure potentially reflecting non-neuronal factors,

452 like skull anatomy, can be reliably separated and is not mixed up in power spectral values  
453 focusing on specific oscillatory phenomena. Although the natural logarithm of term C derived  
454 from formula (1) and (2) ( $\ln C_0$ ) reliably reflects the hypothesized sex differences, the model  
455 could be refined by using alternative intercepts, which were independent from the slopes ( $\ln$   
456  $C_{2.5}$  and  $\ln C_{2.6}$ ) (Fig 4). The latter might constitute an ideal normalization value for NREM  
457 sleep EEG (spectra) in future basic and clinical studies.

458 In addition to the spectral intercepts, the power law functions describing the sleep  
459 EEG spectra appropriately address the issue of the ratio of EEG power at different  
460 frequencies, providing a single measure ( $\alpha$ ), instead of several ones scattered redundantly in  
461 all frequency bins and bands.

462 Last, but not least, spectral peak amplitudes ( $P_{Peak}(f)$ ) are whitened in our approach,  
463 that is, the coloured part of the spectrum is effectively controlled, which might enable  
464 researchers to differentiate random and non-random/oscillatory activities at specific  
465 frequencies.

466 The findings derived from our approach of parametrizing the NREM sleep EEG  
467 spectra clearly supports the robustness and validity of the method presented in this paper,  
468 which was inspired by studies aiming to whiten the spectral power in the sleep spindle  
469 frequency (Gottselig et al., 2002; Geiger et al., 2011). As predicted (H1), age correlates  
470 positively with NREM sleep EEG spectral exponents (Table 1a), indicating that aging is  
471 associated with less steep exponential decay slopes of the Fourier spectra (i.e. less negative  
472 exponents) (Fig 2A). This finding coheres with reports of bandwise power spectral analyses  
473 of NREM sleep EEG, indicating decreased low and increased high frequency activity in the  
474 NREM sleep EEG of healthy aged subjects (Carrier et al., 2001). Moreover, the steepness of  
475 the slope of the linear describing the relationship between the log-amplitude and the log-  
476 frequency of NREM sleep EEG revealed the same age-dependency (Feinberg et al., 1984).



477 Thus, our method is capable of extracting spectral slope information with sufficient precision  
478 and is a valid and simple approach to be used in future (translational) studies. The slope of the  
479 spectrum is basically a measure of the constant ratio between low and high frequency  
480 activities, which was hypothesized to reflect the ratio between inhibition and excitation, the  
481 depth of sleep and/or the level of conscious awareness (Weiss et al., 2011; Gao et al., 2017;  
482 Colombo et al., 2019). Findings might indicate that aged subjects have lower sleep depth, but  
483 might also open new avenues beyond the exclusive focus on sleep slow waves/oscillation  
484 when studying the relationship between aging and sleep. The latter point is supported by our  
485 finding on the lack of a difference in the age-dependency of the NREM sleep EEG spectral  
486 slopes in subjects with average and high intelligence (Table 5). This finding apparently  
487 contrasts the outcomes of our previous report on the significant differences in age-dependent  
488 declines in NREM sleep EEG slow wave/oscillation of average and high IQ subjects. That is  
489 in terms of NREM sleep EEG slow waves high IQ subjects tend to age at a slower pace than  
490 average IQ subjects (Pótári et al., 2017). In spite of the fact that the database we used in the  
491 two studies are the same, the methods (classical spectral analysis vs. spectral exponent  
492 extraction) yield different results. That is, our present findings indicate that average and high  
493 IQ subjects tend to age at a same pace, at least in terms of their NREM sleep EEG spectral  
494 exponents. These contrasting results indicate that our former findings are preferentially  
495 reflecting the age- and IQ-dependency of the NREM sleep EEG slow oscillatory mechanism  
496 per se, but not the random activity and/or the constant ratio of slow and high frequency  
497 activities. The latter could be a subject of aging which is at least partially independent from  
498 the well characterized age-dependent decreases in slow oscillations (Mander et al., 2013) and  
499 is equally present in average and high IQ subjects. Recent findings and considerations suggest  
500 that the spectral slope derived from an electrophysiological signal indicates the ratio of  
501 excitation and inhibition in the underlying neural tissue (Gao et al., 2017). Thus, according to

502 our current findings and previously published modeling data (Gao et al., 2017) aging is  
503 characterized by a relative increase in excitation over inhibition during the state of night time  
504 NREM sleep, and this effect seems to be relatively independent from the decreased slow  
505 oscillation reported in former studies (Mander et al., 2013; Pórtári et al., 2017).

506 Aging was also shown to be associated with decreased sleep spindle frequency activity  
507 and decreased phasic sleep spindles in former studies (Purcell et al., 2017). These findings  
508 cohere with our current report of an age-associated decrease in whitened spectral peak  
509 amplitudes of NREM sleep EEG spindle frequency range (Table 1b). Reports suggest that the  
510 age-dependent decrease in sleep spindles recorded over the prefrontal regions mediates the  
511 cognitive decline in later ages (Mander et al., 2014). Moreover, it was suggested that this  
512 effect reflects the disruption of thalamocortical regulatory mechanisms involved in sleep  
513 spindle rhythmogenesis (Clawson et al., 2017). Thus, our index of whitened NREM sleep  
514 EEG spectral peak amplitude in the spindle frequency range could serve as a simple  
515 biomarker of the neurocognitive aspects of aging.

516 The age-associated increases in the frequency of sleep spindle oscillations (also known  
517 as intraspindle frequencies) were reported in several former reports (e.g. Principe and Smith,  
518 1982), although the largest study did not reveal such changes in adulthood (Purcell et al.,  
519 2017). Our present findings reveal a non-predicted decrease in maximal frontal spectral peak  
520 amplitude in the spindle frequency range of NREM sleep EEG. The range of the spindle  
521 frequency changes clearly indicate a change from the predominant fast (~14 Hz) to  
522 predominant slow (~12 Hz) sleep spindle spectral peaks during aging. That is, our finding  
523 indicates a decrease in relative frontal emergence of fast sleep spindles during aging, rather  
524 than a deceleration of sleep spindles at a rate of 0.5 Hz/decade (Fig 2D). That is, our  
525 minimalistic goals to capture sleep spindle oscillatory activity with just one maximal spectral

526 peak instead of two, resulted in the unexpected deceleration of sleep spindle frequency during  
527 aging in adult subjects.

528 Women were shown to be characterized by significantly higher NREM sleep EEG  
529 spectral intercepts as compared to men. This difference is not seen in the spectral slopes and is  
530 sharpened when using the alternative (“slope-free”) intercepts ( $\ln C_{2.5}$  and  $\ln C_{2.6}$  instead of  $\ln$   
531  $C_0$ ). To the best of our knowledge this is the first report explicitly targeting these issues. We  
532 based our hypothesis on findings suggesting that women vs men differences in EEG power  
533 are largely frequency-independent (Carrier et al., 2001), thus indicating an overall amplitude  
534 effect captured by the term  $C$  in formula (1) and (2). That is, previous reports focusing on  
535 specific frequency ranges and oscillatory phenomena are confounded by overall amplitude  
536 differences in the EEG of women and men. Examples for such potentially confounded  
537 findings are reports on women vs men differences in sleep spindle densities/occurrences.  
538 Spindles detected by fixed thresholds (Crowley et al., 2002; Huupponene et al., 2002) or raw  
539 (non-whitened) spectral power values of the spindle frequency range (Dijk et al., 1989;  
540 Carrier et al., 2001) indicate sex differences (increased sleep spindle density/activity in  
541 women), but are not controlled for overall amplitude differences. It has to be noted however,  
542 that one of the early publications cited above hypothesized that women vs men differences in  
543 sleep EEG spectral power might reflect sex differences in skull thickness (Dijk et al., 1989),  
544 but - at least to our best knowledge - this hypothesis remained largely unexplored from the  
545 electrophysiological point of view. Our current approach considers this issue and provides a  
546 reliable and potentially useful method for controlling non-specific, non-neuronal effects in  
547 EEG amplitude. The estimation of the spectral intercept provides a simple index in the study  
548 of the skull-thickness-EEG power issue in future biophysical, electrophysiological-modeling  
549 studies. Our current findings clearly indicate the lack of sex differences in sleep spindle power  
550 when overall amplitude women vs men differences are controlled (Table 2).

551 Women were shown to be characterized by higher frequency sleep spindle oscillations  
552 as compared to men according to our former study based on the individual adjustment of sleep  
553 spindle frequencies and amplitudes (Ujma et al., 2014). This finding was strengthened by our  
554 current report based on the detection of whitened spectral peak location with .0052 Hz  
555 resolution (Table 3). That is, our current finding strengthens the validity of our spectral  
556 parametrization approach. In addition, the hypotheses suggesting that sleep spindle frequency  
557 is accelerated by either progesterone and its neuroactive, indirect GABA-agonist metabolite  
558 allopregnanolone (Driver et al., 1996) or the progesterone-induced hyperthermia (Deboer,  
559 1998) during the follicular phase of the menstrual cycle in women are indirectly supported by  
560 our present findings. Although our participants were not controlled for menstrual cycle phases  
561 and oral contraceptive use, we can assume that at least some of the female subjects were  
562 examined during the follicular phase of their menstrual cycle. Furthermore, oral contraceptive  
563 use involve the intake of progestagenic compounds, which might induce some of the neural  
564 effects of endogenous progesterone in naturally cycling women.

565 Here we reveal a positive correlation between whitened spectral peak amplitude of  
566 sleep spindle frequency activity during NREM sleep and IQ in women, but not in men (Table  
567 4; Fig 3). Intelligence was shown to be reflected in the intensity (amplitude and/or density) of  
568 phasic sleep spindle events or alternatively in the spectral power of sleep spindle frequency  
569 activity during NREM sleep (Bódizs et al., 2005; Ujma et al., 2014, Ujma et al., 2017; Ujma,  
570 2018). In the database we use in our present study a marked sexual dimorphism of this effect  
571 was also revealed: women but not men were shown to be characterized by the sleep spindle  
572 amplitude/power vs IQ correlations (Ujma et al., 2014; Ujma et al., 2017). Although this latter  
573 effect was not unequivocally reflected in a significant meta-regression between effect size and  
574 % female in the sample in a subsequent metaanalysis, here we refer to it because convergent  
575 findings obtained by different methods used on the same dataset are an issue of validity of the

576 methods. That is, we reproduced the positive sleep spindle vs. IQ correlation in women by  
577 using a linear fitting approach to the log-log spectra of NREM sleep and a concurrent  
578 whitening of spectral peaks, without assumptions on time-domain sleep spindle features.  
579 Again, this finding might strengthen our views on the reliability of the method of analyzing  
580 the constant, the slope and the (whitened) peak attributes of the NREM sleep EEG in human  
581 subjects.

582         Among the shortcomings of our work we would emphasize the lack of slow vs fast  
583 sleep spindle differentiation by the current version of our method, as well as the fact that we  
584 disregarded low frequency power ( $< 2$  Hz) when fitting the slopes. Fitting of two slightly  
585 overlapping spectral peaks instead of just one, would increase considerably the complexity of  
586 the approach, whereas our intention was to keep the process as simple and intuitive as  
587 possible. Moreover, we intended to follow the already published method of finding the  
588 maximal peak in the spindle frequency range and correlating its amplitude/power with  
589 neurological-clinical and cognitive data (Gottselig et al., 2002; Geiger et al., 2011). Similarly,  
590 the potential and largely unpredictable contamination of low frequency power with sweating  
591 artefacts, as well as the high-pass filtering effects of gold-coated electrodes (Vanhatalo et al.,  
592 2005) we used in our studies precluded us from a precise measurement of the power law  
593 scaling at low frequencies below 2 Hz.

594         In sum, the parametrization of NREM sleep EEG of healthy adult subjects by relying  
595 on the power law scaling behavior of the electrical activity of the brain, as well as by  
596 completing this statistical property with the prominent spectral peak at the sleep spindle  
597 range, provides an integral method of describing and characterizing individual differences in  
598 sleep and cognition. Here we show, that most of the features of NREM sleep EEG can be  
599 efficiently compressed in the spectral intercepts, slopes and peaks, at least in terms of  
600 demographic (age, sex) and cognitive (IQ) correlates of sleep. It remains to be determined, if

601 state-dependent changes, like overnight sleep dynamics and or sleep regulatory mechanisms  
602 can be appropriately described by these integrative parameters of NREM sleep. In addition,  
603 further studies are needed for an adequate handling of multiple spectral peaks and low  
604 frequency (< 2 Hz) oscillations in the non-full-band EEG.

605

## 606 **Methods**

### 607 **Subjects/databases**

608 Data was combined from multiple databases (Max Planck Institute of Psychiatry,  
609 Munich, Germany; Institute of Behavioural Sciences of Semmelweis University, Budapest,  
610 Hungary) for this retrospective multicenter study (Ujma et al., 2017; Ujma et al., 2019).  
611 Polysomnography data were recorded from 175 participants (81 females, 94 males, mean age  
612 29.57 years, age range 17–60 years) and IQ scores were measured for 149 participants (68  
613 females, 81 males, mean age 29.23 years, age range 17–60 years). Volunteers were recruited  
614 also via Mensa Germany and Mensa Hungary to increase the number of highly intelligent  
615 individuals. As some of the participants have missing data of some electrodes and/or IQ  
616 scores the data numbers from which the statistical analysis was conducted are always reported  
617 in the results.

618 Based on self-reports, none of the participants had a history of psychiatric or  
619 neurological disorders. Alcohol consumption was restricted before recording, but a small  
620 amount of caffeine (max. 2 cups of coffee before noon) was allowed to the participants. Based  
621 on self reports 8 participants were light or moderate smokers. Data were combined from  
622 multiple databases (Max Planck Institute of Psychiatry, Munich, Germany; Institute of  
623 Behavioural Sciences of Semmelweis University, Budapest, Hungary). The experiment was  
624 conducted in full accordance with the World Medical Association Helsinki Declaration and

625 all applicable national laws and it was approved by the institutional review board, the Ethical  
626 Committee of the Semmelweis University, Budapest, or the Ludwig Maximilian University,  
627 Munich.

628

### 629 **Psychometric intelligence**

630 Standardized nonverbal intelligence tests were recorded from 149 participants: 70 of  
631 them completed the Culture Fair Test (CFT) and 39 of them completed the Raven Advanced  
632 Progressive Matrices (Raven APM) test. 40 participants completed both tests. These tests  
633 have been shown to similarly measure abstract pattern completion and are particularly good  
634 measures of the general factor of intelligence. A composite raw intelligence test score was  
635 calculated, expressed as a Raven equivalent score (RES). RES for Raven APM tests was  
636 equal to the actual raw test score, whereas RES of the CFT test raw scores were equal to the  
637 Raven APM score corresponding to the IQ percentile derived from CFT performance and the  
638 age of the participant. Scores were averaged for participants who completed both tests.  
639 Standardization of APM was applied according to 1993 Des Moines (Iowa). Based on their  
640 mean IQ score, the sample was split into an average (AIQ:  $88 < IQ < 120$ ;  $\overline{IQ} = 106.9$ ;  $N =$   
641  $85$ ) and a high intelligence (HIQ:  $120 \leq IQ < 156$ ;  $\overline{IQ} = 130.38$ ;  $N = 64$ ) subgroup (see  
642 Pótári et al., 2017).

643

### 644 **Polysomnography recordings**

645 Detailed data recording procedures and power spectral analysis are also reported in the  
646 study of Ujma et al. (2019). Sleep data were recorded on two consecutive nights by standard  
647 polysomnography including EEG, electro-oculography (EOG), electrocardiography (ECG)



648 and bipolar submental electromyography (EMG). EEG channels were placed according to the  
649 international 10–20 system (Fp1, Fp2, F3, F4, Fz, F7, F8, C3, C4, Cz, P3, P4, T3, T4, T5, T6,  
650 O1, O2 and left and right mastoids). Impedances for the EEG electrodes were kept below 8  
651 k $\Omega$ . The sampling frequency was either 249 Hz, 250 Hz or 1024 Hz, depending on recording  
652 site (Supplementary table 1). All recordings were referenced to the mathematically linked  
653 mastoids. Data were offline re-referenced to the average of the mastoid signals and notch  
654 filtered at 50 Hz. Electrodes excluded from the analysis due to artifacts and/or recording  
655 failures were treated as missing data. The number missing data for the total 175 participants is  
656 reported in Supplementary Table 2, separately for each electrode. Recordings of the first night  
657 were used for habituation and therefore were not included in further analyses. Sleep data of  
658 the second night in the laboratory were scored for sleep-waking states and stages according to  
659 standard AASM criteria on a 20-sec basis (Iber et al., 2007) by an expert. Furthermore,  
660 artefactual segments were marked on a 4-sec basis and excluded from further analyses.

661

## 662 **Power spectral analysis**

663 Power spectral densities were calculated for the NREM (N2 and N3) sleep, in .25 Hz  
664 bins from 0 Hz to the Nyquist frequency ( $f_{Nyquist}$ ) by relying on 4 s Hanning-tapered, non-  
665 artefactual windows. A 50% overlap was used for consecutive windows, whereas mixed-radix  
666 FFT calculating power spectral densities. Power spectral densities from all 4 s windows were  
667 then averaged. As data were recorded with different EEG devices producing different analog  
668 filter characteristics, average power spectral densities were corrected as follows: An analog  
669 waveform generator was connected to the C3 and C4 electrode positions of all EEG devices  
670 and sinusoid signals of various frequencies (0.05 Hz, every 0.1 Hz between 0.1–2 Hz, every 1  
671 Hz between 2–20 Hz, every 10 Hz between 10–100 Hz) were generated with 40 and 355  $\mu$ V  
672 amplitudes. The amplitude reduction rate of each recording system at each frequency was

673 determined by calculating the proportion between digital (measured) and analog (generated)  
674 amplitudes of sinusoid signals at the corresponding frequency. The amplitude reduction rate  
675 was averaged for the 40 and 355  $\mu\text{V}$  at each frequency. The reduction rate at the intermediate  
676 frequencies were interpolated by spline interpolation. The measured power spectral density  
677 values were corrected with the device-specific amplitude reduction rate by dividing the  
678 original value with the squared amplitude reduction rate at the corresponding frequency  
679 according to previous suggestions (Achermann and Borbély, 1997; Vasko et al., 1997).

680

### 681 **Estimation of the spectral intercepts and slopes**

682 The power law function (formula (2)) was transformed to one which fits in the double  
683 logarithmic plots as follows (Fig. 1C):

$$684 \ln P(f) = \ln C + \alpha \ln f + \ln P_{Peak}(f) \quad (3)$$

685 This means that the natural logarithm of spectral power ( $P$ ) is expressed as a linear function of  
686 the natural logarithm of frequency ( $f$ ). In addition, there are two terms in the equation: the  
687 natural logarithm of the constant ( $C$ ) and the natural logarithm of peak power ( $P_{Peak}$ , see Fig  
688 1). If the latter equals 1 ( $P_{Peak} = 1$ ), that is, there is no peak at a given frequency  $f$ , the value is  
689 0 ( $\ln 1 = 0$ ). The logarithmic frequency scale inherently induces increasing data density at  
690 higher frequencies. Thus, a linear fit to this data would induce a strong bias against low  
691 frequency bins, which would contribute less to the determination of slopes compared to the  
692 higher frequency bins. In order to manage this problem and obtain an equal distribution of the  
693 data points, power values were interpolated up to the smallest frequency step (.0052 Hz) by  
694 the piecewise cubic Hermite interpolation method. In the next step a linear was fitted to the 2–  
695 48 Hz frequency range of this equidistant log-log plot, excluding the 6.0052–17.9948 Hz  
696 frequency range corresponding to the alpha and spindle bands (in order to avoid those parts of

697 the NREM sleep EEG spectra which are characterized by non-random, oscillatory activities as  
698 well). This part of our procedure was inspired by two former studies using a similar approach  
699 for whitening of the sleep spindle spectra (Gottselig et al., 2002; Geiger et al., 2011). The  
700 slope of the linear is  $\alpha$ , whereas its intercept is  $\ln C$ .

701

## 702 **Estimation of the spectral peak frequencies**

703 Spectral peak frequency was determined in the 9–18 Hz range, separately for each  
704 EEG derivation by automatically defining local maxima in mathematical terms. That is, we  
705 used the first derivative test in order to find the critical points, followed by the second  
706 derivative test to differentiate local maxima and minima. A spectral peak was accepted if the  
707 first order derivative was zero and the second order derivative was negative. Calculations  
708 were performed as follows: a second-degree polynomial curve fitting was performed using all  
709 sets of successive bin triplets (.75 Hz), with an overlap of 2 bins (.5 Hz) in the 9–18 Hz range  
710 resulting in equations of the following type:

$$711 \quad P(f) = af^2 + bf + c \quad (4)$$

712  $P$ : power

713  $f$ : frequency (9–18 Hz)

714  $a$ ,  $b$ , and  $c$ : fitted parameters.

715 The first derivative of these functions were calculated for each triplet, resulting in:

$$716 \quad P'(f) = 2af + b \quad (5)$$

717 The slope of the function described in formula (5) is  $2a$ , which was considered as the  
718 derivative at the middle of the triplets, resulting in the first derivative function of the spectra.

719 The procedure was repeated for calculating the second derivatives: in this case the first order  
720 derivative function served as an input for fitting the quadratic polynomials.

721 Zero-crossings of the first derivatives were determined by spline interpolation  
722 (interpolating the series between the bins of .25 Hz). In addition, the second derivative was  
723 interpolated by the spline method at each detected zero crossing of the first derivatives. The  
724 cases which were characterized by the co-occurrences of the two criteria below were  
725 considered as spectral peak frequencies:

$$726 \quad P'(f) = 0 \quad (6.1)$$

$$727 \quad P''(f) < 0 \quad (6.2)$$

728

### 729 **Estimation of the spectral peak amplitudes**

730 Spectral power at peak frequencies were estimated by spline interpolation of the  
731 double logarithmic plots of the power spectra. The spectral peak amplitude was then whitened  
732 by subtracting the estimated power based on the fitted linear function from the coloured peak  
733 power:

$$734 \quad \ln P_{Peak}(f) = \ln P(f) - (\ln C + \alpha \ln f) \quad (7)$$

735 In order to avoid negative amplitudes due to the logarithmic scale, the power values were  
736 shifted for being all positive before this subtraction by adding a constant. This latter step was  
737 applied for the calculation of the amplitude measures only. As multiple spectral peaks were  
738 detected for some of the participants/EEG derivations, the one with the largest amplitude was  
739 determined and used in this study. If no spectral peak was found in the spindle frequency  
740 range, peak values were considered as missing data (see Table 5.). Data analysis was  
741 performed by Matlab R2018b (Mathworks Inc.).

742

### 743 **Statistical analyses**

744 Goodness of fit of the linear to the equidistant log-log spectral data was assessed by  
745 Pearson product moment correlations, which were Fisher Z-transformed, averaged and back-  
746 transformed according to Silver and Dunlap (1987). Last, but not least the resulting average  
747 R-value were squared in order to determine the shared variance. Standard deviation (SD) was  
748 assessed from the Fisher-Z-transformed dataset, and the resulting value was back-transformed  
749 as well.

750 We used parametric tests (Pearson correlation, independent sample t-test) on normally  
751 distributed data and non-parametric tests (Spearman's rank correlation, Mann-Whitney U test)  
752 when the distribution of the data was not Gaussian. The normality of the distributions was  
753 analysed by Shapiro-Wilk tests. In order to control Type 1 statistical errors due to multiple  
754 electrodes/hypothesis, we used a version of the Descriptive Data Analysis (DDA) protocol  
755 (Abt, 1987) adapted for neurophysiological data (Abt, 1990; Duffy, 1990). This procedure  
756 tests the global null hypothesis ("all individual null hypotheses in the respective region are  
757 true") at level .05, against the alternative that at least one of the null hypotheses is wrong.  
758 DDA considers the intercorrelations between the different electrodes and is based on defining  
759 Rürger's areas (Rürger, 1978), which are sets of spatially contingent conventionally  
760 (descriptively) significant ( $p < .05$ ) results. The global significance of the Rürger area means  
761 that at least  $1/3$  of the descriptive significances are significant at a  $p = .05/3 = .017$  and/or  $1/2$   
762 of the descriptive significances are significant at  $p = .05/2 = .025$ . We used both criteria  
763 simultaneously (the "and" operator) in this study. In order to obtain a better localization of  
764 regions with significant correlations, associations between NREM sleep EEG spindle  
765 frequency whitened spectral peak amplitudes and IQ were represented by significant  
766 probability maps (Hassainia et al., 1994).

767

## 768 **Funding**

769 Research supported by the Hungarian Medical Research Council (ETT-162/2003;  
770 <https://ett.aeek.hu/en/secretariat/>), the Hungarian National Research, Development and  
771 Innovation Office (K-128117; <https://nkfih.gov.hu/about-the-office>) the Higher Education  
772 Institutional Excellence Program of the Ministry of Human Capacities in Hungary, within the  
773 framework of the Neurology thematic program of the Semmelweis University  
774 (<http://semmelweis.hu/english/>), the Netherlands Organization for Scientific Research (NWO;  
775 <https://www.nwo.nl/en>), the European Cooperation in Science and Technology (COST Action  
776 CA18106; <https://www.cost.eu/>), as well as the general budgets of the Institute of Behavioural  
777 Sciences, Semmelweis University (<http://semmelweis.hu/magtud/en/>) and the Max Planck  
778 Institute of Psychiatry (<https://www.psych.mpg.de/en>). The funders had no role in study  
779 design, data collection and analysis, decision to publish, or preparation of the manuscript.

780

## 781 **Acknowledgements**

782 We would like to thank Mensa Germany and Mensa Hungary for their help in volunteer  
783 recruitment.

784

## 785 **References**

786 Abt K. Descriptive data analysis: a concept between confirmatory and exploratory data analysis.  
787 *Methods Inf Med.* 1987;26(02):77–88. doi: 10.1055/s-0038-1635488

- 788 Abt K. Statistical aspects of neurophysiologic topography. *J Clin Neurophysiol*. 1990;7(4):519–  
789 534. doi: 10.1097/00004691-199010000-00007
- 790 Achermann P, Borbély AA. Low-frequency (< 1 Hz) oscillations in the human sleep  
791 electroencephalogram. *Neuroscience*. 1997;81(1):213–222. doi: 10.1016/S0306-  
792 4522(97)00186-3
- 793 Bódizs R, Kis T, Lázár AS, Havrán L, Rigó P, Clemens Z, et al. Prediction of general mental  
794 ability based on neural oscillation measures of sleep. *J Sleep Res*. 2005;14(3):285–292.  
795 doi: 10.1111/j.1365-2869.2005.00472.x
- 796 Bódizs R, Gombos F, Kovács I. Sleep EEG fingerprints reveal accelerated thalamocortical  
797 oscillatory dynamics in Williams syndrome. *Res Dev Disabil*. 2012;33(1):153–164. doi:  
798 10.1016/j.ridd.2011.09.004
- 799 Borbély AA, Baumann F, Brandeis D, Strauch I, Lehmann D. Sleep deprivation: effect on sleep  
800 stages and EEG power density in man. *Electroencephalogr Clin Neurophysiol*.  
801 1981;51(5):483–495. doi: 10.1016/0013-4694(81)90225-x
- 802 Campbell IG, Grimm KJ, de Bie E, Feinberg I. Sex, puberty, and the timing of sleep EEG  
803 measured adolescent brain maturation. *Proc Natl Acad Sci U S A*. 2012;109(15):5740–  
804 5743. doi: 10.1073/pnas.1120860109
- 805 Carrier J, Land S, Buysse DJ, Kupfer DJ, Monk TH. The effects of age and gender on sleep  
806 EEG power spectral density in the middle years of life (ages 20-60 years old).  
807 *Psychophysiology*. 2001;38(2):232–242. doi: 10.1111/1469-8986.3820232
- 808 Clawson BC, Durkin J, Aton SJ. Form and function of sleep spindles across the lifespan. *Neural*  
809 *Plast*. 2016;2016:6936381. doi: 10.1155/2016/6936381
- 810 Colombo MA, Napolitani M, Boly M, Gosseries O, Casarotto S, Rosanova M, et al. The spectral  
811 exponent of the resting EEG indexes the presence of consciousness during



- 812 unresponsiveness induced by propofol, xenon, and ketamine. *Neuroimage*.  
813 2019;189:631–644. doi: 1.1016/j.neuroimage.2019.01.024.
- 814 Crowley K, Trinder J, Kim Y, Carrington M, Colrain IM. The effects of normal aging on sleep  
815 spindle and K-complex production. *Clin Neurophysiol*. 2002;113(10):1615–1622. doi:  
816 10.1016/s1388-2457(02)00237-7
- 817 Deboer T. Brain temperature dependent changes in the electroencephalogram power spectrum  
818 of humans and animals. *J Sleep Res*. 1998;7(4):254–262. doi: 10.1046/j.1365-  
819 2869.1998.00125.x
- 820 Dijk DJ, Beersma DG, Bloem GM. Sex differences in the sleep EEG of young adults: visual  
821 scoring and spectral analysis. *Sleep*. 1989;12(6):500–507. doi: 10.1093/sleep/12.6.500
- 822 Driver HS, Dijk DJ, Werth E, Biedermann K, Borbély AA. Sleep and the sleep  
823 electroencephalogram across the menstrual cycle in young healthy women. *J Clin*  
824 *Endocrinol Metab*. 1996;81(2):728–735. doi: 10.1210/jcem.81.2.8636295
- 825 Duffy FH, Jones K, Bartels P, Albert M, McAnulty GB, Als H. Quantified neurophysiology  
826 with mapping: statistical inference, exploratory and confirmatory data analysis. *Brain*  
827 *Topogr*. 1990;3(1):3–12. doi: 10.1007/bf01128856
- 828 Feinberg I, March JD, Fein G, Aminoff MJ. Log amplitude is a linear function of log frequency  
829 in NREM sleep eeg of young and elderly normal subjects. *Electroencephalogr Clin*  
830 *Neurophysiol*. 1984;58(2):158–116. doi: 10.1016/0013-4694(84)90029-4
- 831 Freeman WJ, Holmes MD, West GA, Vanhatalo S. Fine spatiotemporal structure of phase in  
832 human intracranial EEG. *Clin Neurophysiol* 2006;117(6):1228–1243. doi:  
833 10.1016/j.clinph.2006.03.012
- 834 Freeman WJ, Zhai J. Simulated power spectral density (PSD) of background electrocorticogram  
835 (ECoG). *Cogn Neurodyn*. 2009;3(1):97–103. doi: 1.1007/s11571-008-9064-y

- 836 Gao R, Peterson EJ, Voytek B. Inferring synaptic excitation/inhibition balance from field  
837 potentials. *Neuroimage* 2017;158:70–78. doi: 10.1016/j.neuroimage.2017.06.078
- 838 Geiger A, Huber R, Kurth S, Ringli M, Jenni OG, Achermann P. The sleep EEG as a marker of  
839 intellectual ability in school age children. *Sleep*. 2011;34(2):181–189. doi:  
840 10.1093/sleep/34.2.181
- 841 Gottselig JM, Bassetti CL, Achermann P. Power and coherence of sleep spindle frequency  
842 activity following hemispheric stroke. *Brain*. 2002;125(Pt 2):373–383. doi:  
843 10.1093/brain/awf021
- 844 Hassainia F, Petit D, Montplaisir J. Significance probability mapping: the final touch in t-  
845 statistic mapping. *Brain Topogr*. 1994;7(1):3–8. doi: 10.1007/bf01184832
- 846 Huupponen E, Himanen SL, Värri A, Hasan J, Lehtokangas M, Saarinen J. A study on gender  
847 and age differences in sleep spindles. *Neuropsychobiology*. 2002;45(2):99–105. doi:  
848 10.1159/000048684
- 849 Iber C, Ancoli-Israel S, Chesson A, Quan SF, eds. *The AASM manual for the scoring of sleep*  
850 *and associated events: rules, terminology, and technical specification*, 1st ed.  
851 Westchester, IL: American Academy of Sleep Medicine, 2007.
- 852 Kaskie RE, Ferrarelli F. Sleep disturbances in schizophrenia: what we know, what still needs  
853 to be done. *Curr Opin Psychol*. 2019;34:68–71. doi: 1.1016/j.copsyc.2019.09.011.
- 854 Lázár AS, Lázár ZI, Bódizs R. Frequency Characteristics of Sleep. In: *Oxford Handbook of*  
855 *EEG frequency*. (in press)
- 856 Looker AC, Melton LJ 3rd, Harris T, Borrud L, Shepherd J, McGowan J. Age, gender, and  
857 race/ethnic differences in total body and subregional bone density. *Osteoporos Int*.  
858 2009;20(7):1141–1149. doi: 10.1007/s00198-008-0809-6

- 859 Mander BA, Rao V, Lu B, Saletin JM, Lindquist JR, Ancoli-Israel S, et al. Prefrontal atrophy,  
860 disrupted NREM slow waves and impaired hippocampal-dependent memory in aging.  
861 Nat Neurosci. 2013;16(3):357–364. doi: 10.1038/nn.3324
- 862 Mander BA, Rao V, Lu B, Saletin JM, Ancoli-Israel S, Jagust WJ, et al. Impaired prefrontal  
863 sleep spindle regulation of hippocampal-dependent learning in older adults. Cereb  
864 Cortex 2014;24(12):3301–3309. doi: 10.1093/cercor/bht188
- 865 Nicolas A, Petit D, Rompré S, Montplaisir J. Sleep spindle characteristics in healthy subjects  
866 of different age groups. Clin Neurophysiol. 2001;112(3):521–527. doi: 10.1016/s1388-  
867 2457(00)00556-3
- 868 Olbrich E1, Landolt HP, Achermann P. Effect of prolonged wakefulness on  
869 electroencephalographic oscillatory activity during sleep. J Sleep Res. 2014;23(3):253–  
870 260. doi: 10.1111/jsr.12123.
- 871 Pereda E, Gamundi A, Rial R, Gonzalez J. Non-linear behaviour of human EEG: fractal  
872 exponent versus correlation dimension in awake and sleep stages. Neurosci Lett.  
873 1998;250(2):91–94. doi: 10.1016/s0304-3940(98)00435-2
- 874 Pótári A, Ujma PP, Konrad BN, Genzel L, Simor P, Körmendi J, et al. Age-related changes in  
875 sleep EEG are attenuated in highly intelligent individuals. Neuroimage. 2017;146:554–  
876 560. doi: 1.1016/j.neuroimage.2016.09.039
- 877 Principe JC, Smith JR. Sleep spindle characteristics as a function of age. Sleep. 1982;5:73–84.  
878 doi: 10.1093/sleep/5.1.73
- 879 Purcell SM, Manoach DS, Demanuele C, Cade BE, Mariani S, Cox R, et al. Characterizing  
880 sleep spindles in 11,630 individuals from the National Sleep Research Resource. Nat  
881 Commun. 2017;8:1593. doi: 1.1038/ncomms1593.

- 882 Ruger B. Das maximale Signifikanzniveau des tests: “Lehne  $H_0$  ab, wenn  $k$  unter  $n$  gegebene  
883 Tests zur ablehnung fuhren”. *Metrika* 1978;25:171–178. doi: 10.1007/bf02204362
- 884 Silver NC, Dunlap WP. Averaging correlation coefficients: Should Fisher’s  $z$  transformation  
885 be used? *J Appl Psychol.* 1987;72(1):146–148. doi: 10.1037/0021-9010.72.1.146
- 886 Tarokh L, Rusterholz T, Achermann P, Van Dongen HP. The spectrum of the non-rapid eye  
887 movement sleep electroencephalogram following total sleep deprivation is trait-like. *J*  
888 *Sleep Res.* 2015;24(4):360–363. doi: 10.1111/jsr.12279.
- 889 Tinguely G, Finelli LA, Landolt HP, Borbely AA, Achermann P. Functional EEG topography  
890 in sleep and waking: state-dependent and state-independent features. *Neuroimage.*  
891 2006;32(1):283–292.
- 892 Ujma PP, Konrad BN, Genzel L, Bleifuss A, Simor P, Potari A, et al. Sleep spindles and  
893 intelligence: evidence for a sexual dimorphism. *J Neurosci.* 2014;34(49):16358–16368.  
894 doi: 1.1523/JNEUROSCI.1857-14.2014
- 895 Ujma PP, Konrad BN, Gombos F, Simor P, Potari A, Genzel L, et al. The sleep EEG spectrum  
896 is a sexually dimorphic marker of general intelligence. *Sci Rep.* 2017;7(1):1807. doi:  
897 10.1038/s41598-017-18124-0
- 898 Ujma PP. Sleep spindles and general cognitive ability – A meta-analysis. *Sleep Spindles &*  
899 *Cortical Up States*, 2018. doi: 10.1556/2053.2.2018.01
- 900 Ujma PP, Konrad BN, Simor P, Gombos F, Kormendi J, Steiger A, et al. Sleep EEG functional  
901 connectivity varies with age and sex, but not general intelligence. *Neurobiol Aging.*  
902 2019;78:87–97. doi: 10.1016/j.neurobiolaging.2019.02.007
- 903 Ujma PP, Simor P, Steiger A, Dresler M, Bodizs R. Individual slow-wave morphology is a  
904 marker of aging. *Neurobiol Aging.* 2019;80:71–82. doi:  
905 10.1016/j.neurobiolaging.2019.04.002

- 906 Ujma PP, Bódizs R, Dresler M. Sleep and intelligence: critical review and future directions.  
907 *Curr Opin Behav Sci.* 2020;33:109–117. doi: 10.1016/j.cobeha.2020.01.009
- 908 Vanhatalo S, Voipio J, Kaila K. Full-band EEG (FbEEG): an emerging standard in  
909 electroencephalography. *Clin Neurophysiol.* 2005;116(1):1–8. doi:  
910 10.1016/j.clinph.2004.09.015
- 911 Vasko RC Jr, Brunner DP, Monahan JP, Doman J, Boston JR, el-Jaroudi A, et al. Power spectral  
912 analysis of EEG in a multiple-bedroom, multiple-polygraph sleep laboratory. *Int J Med*  
913 *Inform.* 1997;46(3):175–184. doi: 10.1016/s1386-5056(97)00064-6
- 914 Weiss B, Clemens Z, Bódizs R, Halász P. Comparison of fractal and power spectral EEG  
915 features: Effects of topography and sleep stages. *Brain Res Bull.* 2011;84(6):359–375.  
916 doi: 10.1016/j.brainresbull.2010.12.005
- 917 Welch PD. The use of Fast Fourier Transform for the estimation of power spectra: A method  
918 based on time averaging over short, modified periodograms. *IEEE Transactions on*  
919 *Audio and Electroacoustics.* 1967;15(2):70–73. doi: 10.1109/TAU.1967.1161901
- 920
- 921

922 **Supporting information**

923 *Supplementary table 1. Technical details of the recordings in different subsamples included in*  
 924 *the present investigation*

Subsample	Recording apparatus	Precision (bit)	Hardware (firmware) filtering (Hz)	Sampling frequency (Hz/channel)	N
Budapest-I	Flat Style Lamont Headbox, HBX32-SLP preamplifier	12	0.5–70	249	43
Budapest-II	Brain-Quick BQ132S Headbox and EEG Amplifier	12	0.33–1500 (0.33–450)	4096 (decimated to 1024 Hz after filtering by firmware)	19
Münich	Comlab 32 Digital Sleep Lab	8	0.53–70 Hz	250	113

925

926 *Supplementary table 2. The number of missing/artefactual records (EEG) and peak power*  
 927 *values ( $P_{Peak}$ ), separately for each electrode*

	Fp1	Fp2	F3	F4	Fz	F7	F8	C3	C4	Cz	P3	P4	T3	T4	T5	T6	O1	O2
EEG	19	13	10	10	28	31	30	10	9	28	9	9	30	28	30	29	9	10
$P_{Peak}$	32	29	18	18	33	45	43	12	12	29	9	10	59	53	32	33	11	12

928